

Nonlinear Optical Properties of ZnO

Hyeong Seop Shim, Noh Soo Han, Joo Hee Seo, Seung Min Park,* and Jae Kyu Song*

Department of Chemistry, Kyung Hee University, Seoul 130-701, Korea
*E-mail: smpark@khu.ac.kr (S. M. Park), jaeksong@khu.ac.kr (J. K. Song)
Received June 11, 2010, Accepted July 12, 2010

Key Words: ZnO, Second-harmonic generation, Two-photon absorption, Three-photon absorption

Recent advances in material science have led to the production of high quality crystals for II-VI and III-V semiconductors. Among the many II-VI semiconductors available, zinc oxide (ZnO) has attractive properties, such as a wide band gap (3.37 eV) and a large exciton binding energy (60 meV).^{1,2} However, compared to the linear optical properties, there is less understanding of the nonlinear optical properties of ZnO. Some studies of the nonlinear optical responses, such as second-harmonic generation (SHG) and third-harmonic generation (THG), have been reported.³⁻⁷ The nonlinear optical responses supply a deep penetration depth of the probe beam because long excitation wavelengths can be used in two-photon absorption (2PA) and three-photon absorption (3PA).⁵⁻⁹ Despite the importance of competition between harmonic generation (SHG and THG) and multiphoton absorption (2PA and 3PA) for potential applications, there are only a few reports on the simultaneous measurements of harmonic generation and multiphoton absorption.^{5,6} In this Note, the nonlinear optical properties of ZnO were examined by nonresonant optical excitation of femtosecond pulses, which revealed concurrent harmonic generation and multiphoton absorption.

Figure 1(a) shows a typical photoluminescence spectrum of the ZnO bulk powders. The emission peak at 382 nm was assigned to the well-known exciton emission.^{1,2} The absence of visible emission that normally results from defects suggests that the nonlinear optical properties of ZnO can be investigated systematically without the perturbation of defects. Figure 1(b) shows the nonlinear optical responses of ZnO, which were obtained by intensive excitation of the fundamentals such as 800, 750, and 710 nm. The SHGs at 400 and 375 nm, which were twice the photon energy of 800 and 750 nm, were observed along with exciton emission at 382 nm. A small intensity of SHG at 355 nm was also found when the fundamental was tuned to 710 nm. Although the full width at half maxima (FWHMs) of the SHGs at 400, 375, and 355 nm appeared to be different on the wavelength scale, the FWHMs in the photon energy scale were almost identical.

The intensities of the SHGs were not similar in Figure 1(b) because the intensity of SHG at a given time ($I_{2\omega}$) has a dependence on the frequencies of the incident fundamental beam from the following equation.¹⁰

$$I_{2\omega}(\alpha) = \left(\frac{512\pi^3}{A} \right) t_{\omega}^4(\alpha) T_{2\omega}(\alpha) I_{\omega}^2 \frac{\sin^2(\Psi_{SHG}(\alpha))}{[n_{\omega}^2(\alpha) - n_{2\omega}^2(\alpha)]^2} d_{eff}^2(\alpha) \quad (1)$$

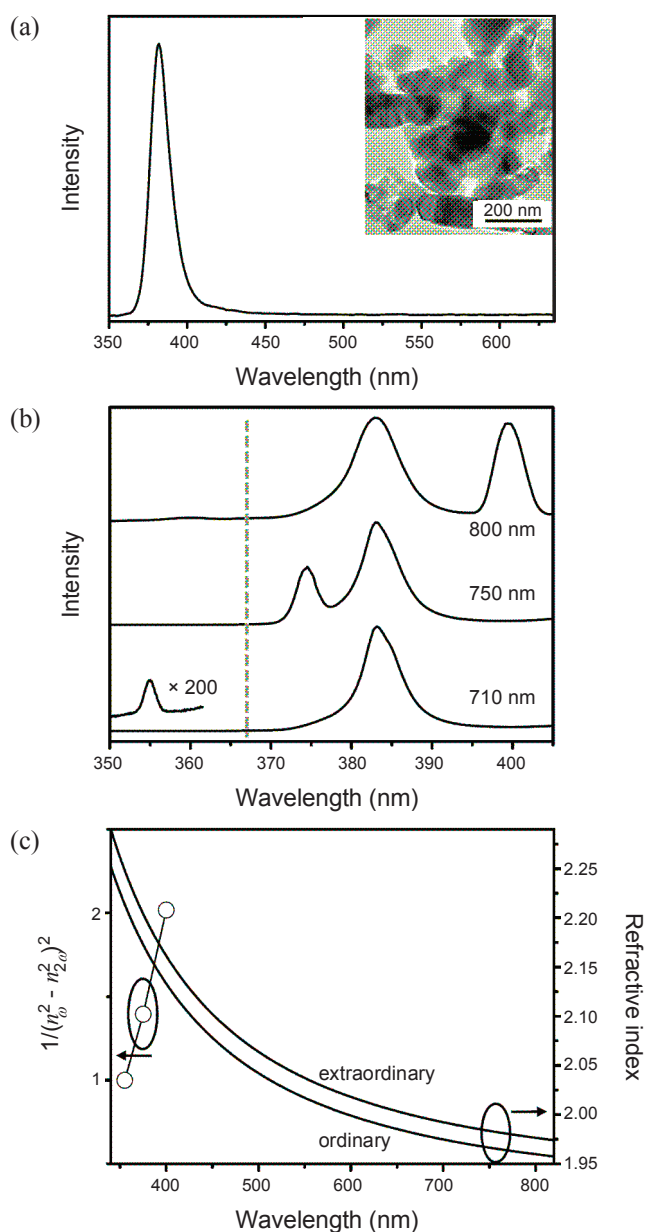


Figure 1. (a) Photoluminescence spectrum of the ZnO powders obtained with a He-Cd laser (325 nm). Inset shows the transmission electron microscopy (TEM) image of the ZnO powders used for the measurements. (b) Emission spectrum of the ZnO powders obtained by intensive excitation of fundamentals, such as 800, 750, and 710 nm. The dotted line indicates the band gap of ZnO. (c) Refractive index and its difference related term as a function of the wavelength.

where α is the incidence angle, A is the fundamental beam transverse area, t_{ω} is the fundamental field transmission coefficient, $T_{2\omega}$ is the second harmonic generation transmission coefficient, I_{ω} is the intensity of the incident fundamental beam, Ψ_{SHG} is the phase factor, n_{ω} and $n_{2\omega}$ are the refractive indices at the fundamental and the second harmonic frequencies, and d_{eff} is the effective susceptibility. Initially, the refractive indices (n_{ω} and $n_{2\omega}$) appeared to play a role in the intensity of SHG because the refractive index had strong frequency (wavelength) dependence. The refractive index on the wavelength was estimated using the Sellmeier model,¹⁰

$$n^2(\lambda) = \frac{E_d E_0}{E_0^2 - E^2} + 1, \quad (2)$$

where E_0 is the single oscillator energy, E_d is the dispersion energy, and E is the photon energy. E_0 and E_d for the ordinary direction are 6.20 and 16.51 eV, respectively, whereas they are 6.08 and 16.52 eV for the extraordinary direction.^{10,11} Both the ordinary and extraordinary refractive indices decreased with increasing wavelength, as shown in Figure 1(c). Therefore, the term related to the difference between the refractive indices ($1/(n_{\omega}^2 - n_{2\omega}^2)^2$) increased with increasing wavelength.

When the refractive index difference was considered, the intensity of SHG should be larger at a longer wavelength. For example, the SHG at 400 nm was expected to be approximately 1.5 times larger than that at 375 nm, which may explain the largest intensity of SHG at 400 nm. However, the difference in refractive index could not give a clear answer to the intensity of SHG at 355 nm, which was too small compared to that expected. Thus, it is noted that the photon energy of SHG at 355 nm is larger than the band gap of ZnO (368 nm, 3.36 eV). In other words, the band gap absorption (the low transmission coefficient, $T_{2\omega}$) might result in a lower intensity of SHG at 355 nm than expected, as found in the SHG at 360 nm,^{12,13} because the photon energy of SHGs is the main difference between the low intensity of SHG at 355 nm and the relatively high intensity at 400 and 375 nm.

The emission spectra were obtained as a function of the excitation intensity to examine SHG and exciton emission in more detail. Figure 2(a) shows that exciton emission and SHG increased nonlinearly, which suggests that both were nonlinear optical responses. The number of photons involved in the nonlinear process (n) was estimated using the following equation,

$$I = cP^n \quad (3)$$

where I is the intensity, c is the constant, and P is the power of the excitation pulse. The logarithmic plots in Figure 2(b) show that n is ~ 2.0 in both nonlinear responses, which confirmed that the band gap excitation for the exciton emission was facilitated by two photons. Therefore, the low intensity of the SHG at 355 nm was attributed to its absorption. Figure 3 shows the emission spectra as a function of the excitation intensities at 750 and 800 nm. The exciton emission and SHG increased nonlinearly by excitation at 750 and 800 nm. On the other hand, the exciton emission increased faster than the SHGs, as shown

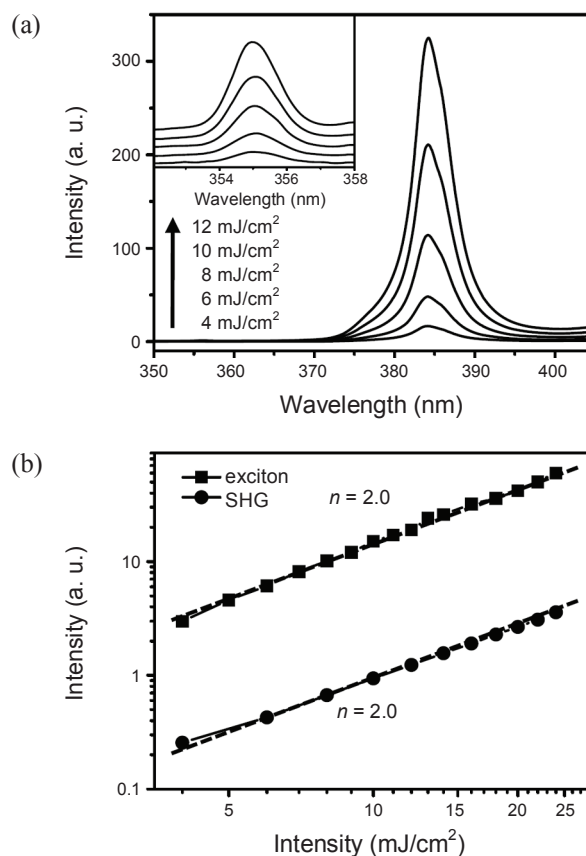


Figure 2. (a) Emission spectra of the ZnO as a function of the excitation intensity at 710 nm. Inset shows the magnified spectra in the regime of second-harmonic generation (SHG). (b) The logarithmic plots of the intensities of exciton emission and SHG.

in Figure 3(c), suggesting different orders of nonlinear optical responses. Figure 4(a) shows the logarithmic plots of the SHG intensities at 355, 375, and 400 nm, which again supports that all the SHGs were two-photon processes ($n \sim 2.0$). On the other hand, the nonlinear processes for exciton emission (band gap excitation) deviated from the two-photon process at the fundamentals of 750 and 800 nm, as shown in Figure 4(b). In addition, the nonlinearity order was not even a constant. In other words, the values of n increased with increasing excitation intensity at 800 and 750 nm, indicating a complicated scheme for band gap excitation. The nonlinearity order increased to 2.9 and 2.4 at 800 and 750 nm, respectively, in the high excitation intensity regime.

In general, a two-photon-induced process, such as SHG, should show a quadratic dependence on the excitation intensity ($n = 2$), whereas a three-photon-induced one showed a cubic dependence ($n = 3$). Thus, the non-integer value of n indicates the coexistence of 2PA and 3PA, as previously suggested.⁵ Indeed, the 2PA process was not expected under normal excitation conditions at 800 and 750 nm because the two-photon energy was less than the band gap of ZnO. However, in intense femtosecond laser excitation, the strong light-matter interaction can induce the 2PA process to some extent.⁶ On the other hand, 3PA can occur without an energy limitation because the three-photon energy was larger than the band gap energy. Nevertheless, the

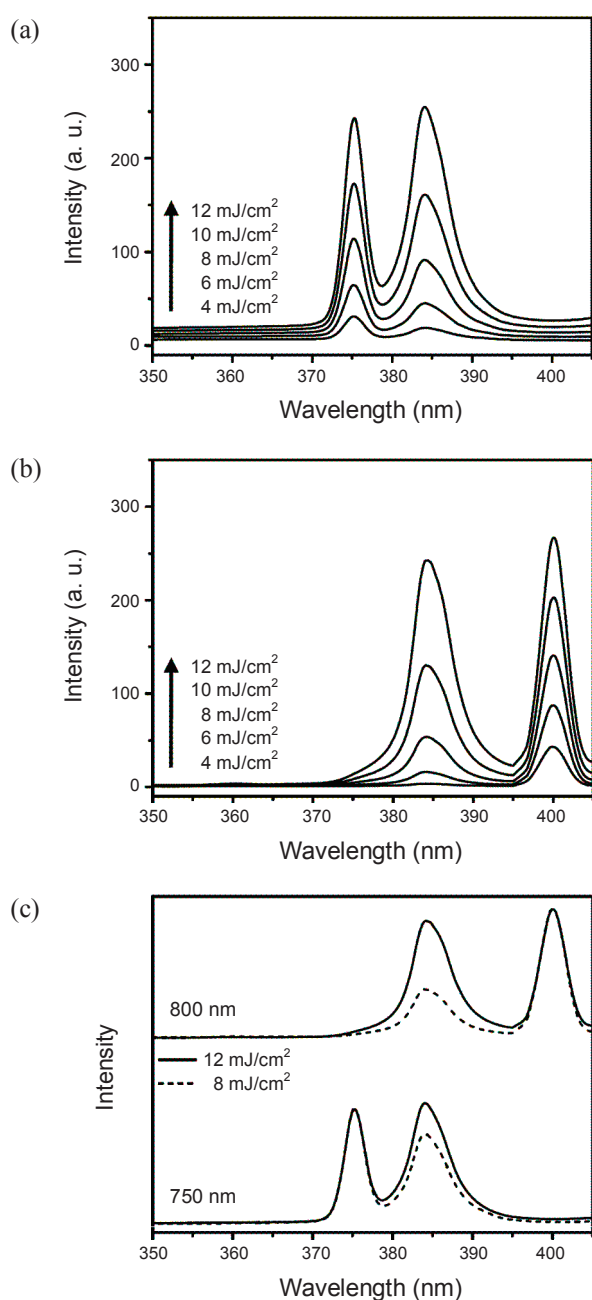


Figure 3. Emission spectra of the ZnO as a function of the excitation intensity of (a) 750 and (b) 800 nm. (c) Emission spectra normalized to the intensity of SHG.

efficiency of the frequency-degenerate 3PA was usually much lower than that of 2PA,⁹ because three photons should be absorbed simultaneously through two virtual states to reach the conduction band in the 3PA process. In other words, the 3PA process should contain two intraband transitions and one interband transition simultaneously, which suggests that 3PA could be observed only at a very high excitation intensity.

In this regard, the change in n suggests that the relative contribution of 3PA in the band gap excitation varies with the excitation intensity. The 3PA process became more important with increasing excitation intensity, where the 3PA process was predominant with $n \sim 2.9$ at the highest excitation intensity

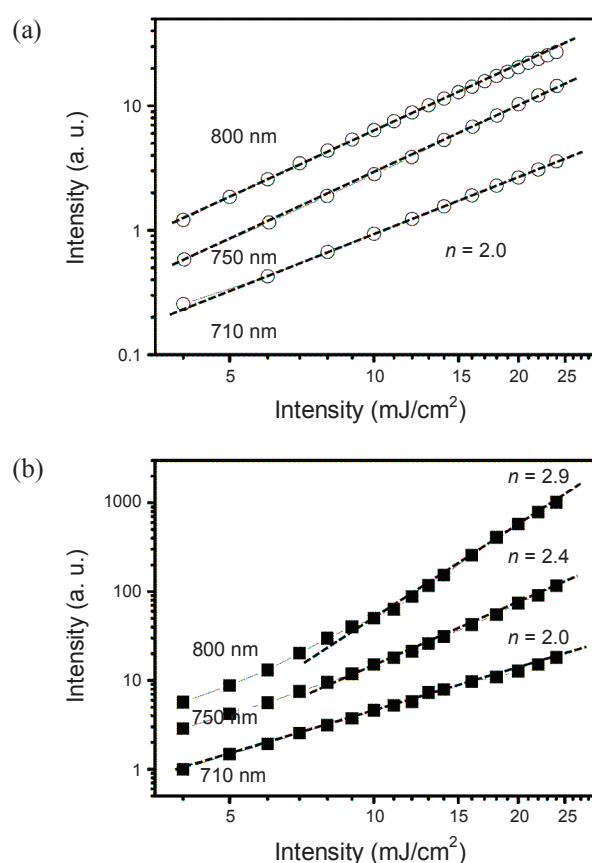


Figure 4. Logarithmic plots of the intensity of (a) SHG and (b) exciton emission.

of 800 nm. At this point, it is not clear why the relative contribution of the 3PA process increased with increasing excitation intensity. One possibility could be attributed to the “excitation intensity dependence”. The 3PA process showed a cubic relationship upon excitation, whereas the 2PA process by a light-matter interaction had a complex dependence on the excitation intensity.⁶ Accordingly, 3PA could become more important with increasing excitation intensity. Another possibility was found at “two-photon-enhanced three-photon absorption”. When the energy states existed inside the band gap as a result of surfaces, defects, and impurities, the inside-gap states may explain the enhancement of the 3PA process. For example, the band gap excitation by the 3PA process was enhanced in ZnSe nanoparticles, when the inside-gap states were in resonance with the two-photon energy.¹⁴ Therefore, the resonance of the inside-gap states with the two-photon energy might facilitate the 3PA process, which can explain the increase in the relative contribution of the 3PA process.

Similarly, the coexistence of 2PA and 3PA processes was observed in the excitation of 750 nm. In addition, the contribution of the 3PA process also increased with increasing excitation intensity. On the other hand, the value of n (~ 2.4) was lower than that of 800 nm, indicating that the 2PA process was not negligible at 750 nm. It appears that the two-photon energy of 750 nm (3.31 eV), which was larger than that of 800 nm (3.10 eV), led more efficient two-photon band gap excitation, even though the 2PA process at 750 nm was enabled by the

light-matter interaction in the intense femtosecond laser field.

In summary, the nonlinear optical properties of ZnO were examined by the nonlinear optical pumping of femtosecond pulses. Exciton emission and SHG were observed by multiphoton excitation, and both showed strong wavelength dependence. This power dependence suggests that exciton emission is affected by 2PA and 3PA, whereas the contribution of each process is also wavelength-dependent.

Experimental Section

The bulk ZnO powders were purchased from Aldrich (#205 532). The nonlinear optical response was measured by exciting the ZnO bulk powders drop-coated on glass substrates by the tunable fundamentals of a cavity-dumped oscillator (710 - 800 nm, Mira/PulseSwitch, Coherent, 1 MHz, 200 fs). Emission was resolved spectrally using a monochromator and detected using a charged coupled device (iDus, Andor).

Acknowledgments. This work was supported by the Kyung Hee University Research Fund in 2008 (KHU-20080535).

References

1. Klingshirn, C. *Phys. Status Solidi B* **2007**, *9*, 3027.
2. Kim, S. Y.; Lee, I. S.; Yeon, Y. S.; Park, S. M.; Song, J. K. *Bull. Korean Chem. Soc.* **2008**, *29*, 1960.
3. Lin, J.-H.; Chen, Y.-J.; Lin, H.-Y.; Hsieh, W.-F. *J. Appl. Phys.* **2005**, *97*, 033526.
4. Wang, G.; Kiehne, G. T.; Wong, G. K. L.; Ketterson, J. B.; Liu, Z.; Chang, R. P. H. *Appl. Phys. Lett.* **2002**, *80*, 401.
5. Han, N. S.; Shim, H. S.; Park, S. M.; Song, J. K. *Bull. Korean Chem. Soc.* **2009**, *30*, 2199.
6. Zhang, C. F.; Dong, Z. W.; You, G. J.; Zhu, R. Y.; Qian, S. X.; Deng, H.; Cheng, H.; Wang, J. C. *Appl. Phys. Lett.* **2006**, *89*, 042117.
7. Petrov, G. I.; Shcheslavskiy, V.; Yakovlev, V. V.; Ozerov, I.; Chelnokov, E.; Marine, W. *Appl. Phys. Lett.* **2003**, *83*, 3993.
8. Zhang, C. F.; Dong, Z. W.; You, G. J.; Qian, S. X.; Deng, H.; Gao, H.; Wang, J. C.; Li, Y. *Appl. Phys. Lett.* **2005**, *87*, 051920.
9. Chon, J. W. M.; Gu, M.; Bullen, C.; Mulvaney, P. *Appl. Phys. Lett.* **2004**, *84*, 4472.
10. Larciprete, M. C.; Haertle, D.; Belardini, A.; Bertolotti, M.; Sarto, F.; Günter, P. *Appl. Phys. B* **2006**, *82*, 431.
11. Karpina, V. A.; Lazorenko, V. I.; Lashkarev, C. V.; Dobrowolski, V. D.; Kopylova, L. I.; Baturin, V. A.; Pustovoytov, S. A.; Karpenko, A. J.; Eremin, S. A.; Lytvyn, P. M.; Ovsyannikov, V. P.; Mazurenko, E. A. *Cryst. Res. Technol.* **2004**, *39*, 980.
12. Voss, T.; Kudyk, I.; Wischmeier, L.; Gutowski, J. *Phys. Status Solidi B* **2009**, *246*, 311.
13. van Vugt, L. K.; Rühle, S.; Ravindran, P.; Gerritsen, H. C.; Kuipers, L.; Vanmaekelbergh, D. *Phys. Rev. Lett.* **2006**, *97*, 147401.
14. Feng, X. B.; Xing, G. C.; Ji, W. *J. Opt. A* **2009**, *11*, 024004.